

A New MTest Beamline  
for the  
1999 Fixed Target Run

C.N. Brown, T.R. Kobilarcik

6 April 2000

**Abstract**

The beamline cryogenic system for the Meson area will not be run for the 1999 fixed target run. The current MTest (MT) beamline relies on cryogenic magnets. A non-cryogenic solution is proposed which can yield up to  $1 \times 10^6$  pions per cycle at 120 GeV/c per  $1 \times 10^{11}$  incident protons at 800 GeV/c.

# Contents

<b>1</b>	<b>Previous (Cryogenic) Configuration</b>	<b>3</b>
<b>2</b>	<b>Proposed Changes</b>	<b>3</b>
2.1	M01 . . . . .	3
2.2	M02 . . . . .	3
2.3	MT5 . . . . .	4
<b>3</b>	<b>Pion Beam</b>	<b>4</b>
3.1	Overview . . . . .	4
3.2	Small Spot . . . . .	5
3.2.1	Monte Carlo . . . . .	5
3.2.2	Nominal Fields . . . . .	5
3.3	Large Spot . . . . .	6
3.3.1	Monte Carlo . . . . .	6
3.3.2	Phase Space Considerations . . . . .	6
3.4	Rates Summary . . . . .	6
<b>4</b>	<b>Radiation</b>	<b>6</b>
4.1	Target . . . . .	6
4.2	Uninteracted Beam . . . . .	7
4.3	Site Boundary Muons . . . . .	8
4.4	Other Meson Beamlines . . . . .	8
<b>5</b>	<b>Results</b>	<b>8</b>
5.1	Small Spot . . . . .	8
5.2	Large Spot . . . . .	9
5.3	Purity . . . . .	9
<b>6</b>	<b>Conclusion</b>	<b>10</b>
<b>7</b>	<b>Tables and Figures</b>	<b>11</b>

## 1 Previous (Cryogenic) Configuration

Initially, MT was produced by inserting a thin target at one of four positions along the three magnets [MW2WD2] which formed the third bend point of the MWest (MW) beamline. These three magnets were on a single power supply, whose current was fixed to deliver 800 GeV/c beam to MW. Thus, the MT momentum was initially selected by changing the production point (and thus the  $B \times L$  seen by the particle), and further selected by the second bend string [MT2WU] of the MT beamline.

During the previous fixed target run, MW was not operated, so a small steel pile was added downstream of MW2WD2 to absorb the uninteracted protons.

Test beam users can place equipment in either of two areas in the Meson Detector Building—these areas are names “MT6 Section 1” (MT6S1) and “MT6 Section 2” (MT6S2). There is additional space behind MT6S2 to build additional enclosures.

## 2 Proposed Changes

Changes need to be made in M01, M02, and MT5. Each enclosure is summarized individually. Refer to figure 1 for a schematic representation of the entire beamline.

### 2.1 M01

The current four-target scheme will be replaced by a single thick target at the upstream end of the Meson Target Train. The target is a 4 inch diameter by 18.5 inch long aluminum billet. The targetting angle will be zero degrees, allowing maximum production.

The change-over will require a minimum amount of work: removing a spool-piece and SWIC, inserting the target, and replacing the SWIC and spool-piece. An aluminum cylinder of the appropriate size has been located.

### 2.2 M02

Refer to figure 2 for this section.

For the upcoming fixed target run, the cryogenic magnets [MW2WD1], which form the second bend point for MW, will be removed; these magnets will be replaced by three EPB dipoles [MT2WD1]. This string will initially momentum-select the secondary beam. Momenta up to 227 GeV/c may be transported.

As previously noted, the current four-target scheme will be replaced by a single thick target at the upstream end of the Meson Target Train.

The beamline will initially be configured for positive secondaries; negative secondaries may be transported by reversing the polarities of all magnets.

Two quadrupoles will be added in M02. The first quadrupole [MT2Q1] is located immediately upstream of the first dipole, and is vertically focusing to increase acceptance. The second quadrupole [MT2Q2] is located immediately after the first dipole. Several quadrupole configurations have been studied—this one was chosen because it maximizes transmission. The MW collimator in the Meson target train serves as a collimator to protect the coils of the first quadrupole.

Uninteracted primary beam will be absorbed between MT2WD1-3 and MT2WD2-1. Ground water calculations and scaling from existing absorbers indicates that adequate shielding is available. Refer to section 4.

A vertical trim magnet will be added immediately downstream of the MT2WD2 string.

All power supplies for the new dipoles and the quadrupoles are extant in the MS2 service building. Bus will be rerouted to the new magnets, but additional power supplies and controls will not be needed. The needed dipoles and quadrupoles have been identified.

## 2.3 MT5

Studies indicate that the brightness of the beam can be doubled by the addition of a doublet in MT5. This doublet, along with a vertical trim magnet, will be added upstream of the final bend. Refer to figure 3.

# 3 Pion Beam

## 3.1 Overview

When the MT beamline was redesigned, the major user was to be E897/BTeV. E897 was interested in a “bright” spot, that is, one with a small core; E897 was to be located in MT6S1. It was also recognized that other users might prefer a larger spot. In discussions with E897, it was agreed that the pion rates would be calculated through a plane located in MT6S1 and normal to the central ray. This plane was divided into four square, concentric, areas (or regions): the “total” region (6” by 6”), a 2” by 2” region, a 1” by 1” region, and a 1/2” by 1/2” region. This allowed E897 to determine how bright the spot was, and allowed other users to judge how large the spot was.

The studies rely heavily on TRANSPORT<sup>1</sup>, TURTLE<sup>2</sup>, MARS<sup>3</sup>, and the Malensek parameterization<sup>4</sup>.

---

<sup>1</sup>Carey, D. C., et al., “Third-Order Transport: A Computer Program for Designing Charged Particle Beam Transport Systems”, Fermilab-Pub-95/069.

<sup>2</sup>Carey, D. C., Fermilab Report NAL-64 (1971).

<sup>3</sup>N.V. Mokhov, “The Mars Code System User’s Guide”, Fermilab-FN-628 (1995).  
O.E. Krivosheev and N.V. Mokhov, “A New MARS and its Applications”, Fermilab-Conf-98/43 (1998).

<sup>4</sup>Malensek, A. J., “Empirical Formula for Thick Target Particle Production”, FN-341 (1981)

The momentum range of the beam is set by current limits in the magnets. The highest momentum possible is 227 GeV/c, which is limited by the EPB string MT2WU. The lowest momentum is limited by regulation of the power supplies—3 GeV/c pions have been transported, but lower momenta have not been investigated.

Two running modes are investigated—a “large spot” mode and a “small spot” mode. The large-spot mode gives a 2.8 cm by 0.6 cm beam spot at the center of MT6S1, while the small-spot mode give a 0.8 cm by 0.2 cm beam spot at the same location. Due to current limits of the final quadrupole doublet, the small-spot mode is limited to momenta up to 150 GeV/c; the large-spot mode may be used for any momentum up to 227 GeV/c. In MT6S1, the yield of the large-spot mode is approximately  $1.4 \times 10^{-5}$  pions (227 GeV/c) per incident proton (that is, per proton incident on the primary target); the yield of the small-spot mode is approximately  $7.2 \times 10^{-6}$  pions (150 GeV/c) per incident proton.

SWIC pictures from the previous run indicate a beam spot of 14 mm FWHM ( $\sigma = 5.9$  mm) horizontal and 7 mm FWHM ( $\sigma = 3.0$  mm) vertical immediately upstream of the proposed target location. Such a beam, incident on 1.2 interaction-length aluminum target was modeled using MARS. The MARS simulation gave  $2.39 \times 10^{-2}$  positive pions at the downstream face of the target per incident proton. The momentum range of the pions was 110 GeV/c to 130 GeV/c. The angular divergence of the beam was 3.63 mradians (RMS). The spatial shape of the beam did not differ markedly from that of the primary beam.

Optimization for each mode was an iterative process involving TRANSPORT and TURTLE. TRANSPORT was used to vary quadrupole gradients and locations, then TURTLE was run to calculate rates.

Due to the large dispersion of the beamline, no configurations gave a momentum bite greater than  $\pm 2\% \Delta p/p$ —in order to save time, this momentum bite was used.

Table 1 summarizes the production, momentum-bite adjustment, and loss due to decay, which must be factored into the final yield.

## 3.2 Small Spot

### 3.2.1 Monte Carlo

Table 2 and figures 4 and 5 characterize the beam in enclosure MT6. Recall that the small-spot mode is good only up to 150 GeV/c.

### 3.2.2 Nominal Fields

Table 3 lists the nominal current, field (or gradient), and type for the MT magnets. 120 GeV/c secondaries are assumed. This mode is limited by MT5Q1 and MT5Q2, which should not be run above 90 amp (this corresponds to 150 GeV/c).

### 3.3 Large Spot

#### 3.3.1 Monte Carlo

Table 4 and figures 6 and 7 characterize the beam in enclosure MT6. Recall that the large-spot mode is used for momenta above 150 GeV/c.

#### 3.3.2 Phase Space Considerations

Using TRANSPORT, the initial beam was varied in angle and momentum-bite until the beam envelope was not occluded by any apertures—refer to figure 8. The Malensek parameterization was integrated over this phase space to obtain particle yields—see table 5. (An advantage to this method is that several species at several production momenta may be quickly calculated).

Reading the number for 120 GeV/c positive pions from the chart (and dividing by  $10^{11}$  protons) gives:

$$1.4 \times 10^{-5} \pi^+ / p$$

This number is in excellent agreement with MARS, which predicts a yield of:

$$1.3 \times 10^{-5} \pi^+ / p$$

### 3.4 Rates Summary

Table 6 lists rates for the large-spot and small-spot modes. Rates are adjusted for production, momentum acceptance, and loss due to decay. We assume  $10^{11}$  protons and a 20 second spill time.

## 4 Radiation

All calculations in this section, unless otherwise stated, assume 800 GeV/c protons, at a rate of  $4.00 \times 10^{11}$  protons per pulse [ppp], 63 pulses per hour, 100 hours per week, and 26 weeks of running per year. This yields an integrated proton intensity of  $6.55 \times 10^{16}$  protons per year.

### 4.1 Target

As previously mentioned, the target is an aluminum billet, 18.5 inches long and 4 inches in diameter. Modeling with MARS indicates that 15.7 GeV of energy will be deposited in the target. This gives a peak temperature rise of 2.3 K in a  $15 \text{ cm}^3$  volume, assuming  $1 \times 10^{12}$  protons instantaneously. Calculations including only conduction across the radial surface and radiation from the ends indicate that the target will not melt. More important, experience with similar targets proves that they will not melt.

The target is contained in a 6 inch diameter beam pipe. This beam pipe has isolation windows on either end. Therefore, any activated air will not escape the pipe.

The model predicts a star density of  $9.0 \times 10^{-6}$  stars per cubic centimeter per proton. Assuming an integrated intensity of  $6.55 \times 10^{16}$  protons per year results in 40% of the allowed tritium limit<sup>5</sup>.

## 4.2 Uninteracted Beam

As previously mentioned, the uninteracted primaries will be absorbed between MT2WD1-3 and MT2WD2-1. Table 7 lists the displacement between the uninteracted primaries and the nominal trajectory for various secondary momenta. Note that for the highest momentum secondaries (227 GeV/c), the primary beam is 78 mm (3.1 inches) off axis—if a 3 inch diameter beam pipe is used in this area, the primary beam dumps 1.6 inches from the edge.

The shielding for the absorber must also accommodate the MC beam, which increase the size of the shielding. This shielding will be built from existing plates from the decommissioned MP target pile—the design<sup>6</sup> requires no fabrication and only two cuts. See figure 9.

MARS was used to model star-density in the surrounding soil for two configurations. In the first configuration, no beam hole is assumed—this is the geometry directly below the absorber. In the second configuration, the amount of steel as a function of azimuthal angle was plotted (accounting for the beam hole), and the minimum amount was chosen.

In the first model, 800 GeV/c protons strike a 22.5 inch radius by 10 foot long steel cylinder. The cylinder is surrounded by 16 inches of concrete. This concrete is surrounded by 10 cm of soil. Refer to figure 9. Cylindrical symmetry was used to increase statistics. The model is cut into 50 cm long slices (in order to determine the area of maximum star density). The distance to the aquifer is assumed to be 46 feet.

The predicted star density in soil is  $(1.56 \pm 0.13) \times 10^{-6} \text{ stars/cm}^3/\text{proton}$ . Assuming an integrated intensity of  $6.55 \times 10^{16}$  protons per year results in 15% of the allowed tritium limit<sup>7</sup>.

In the second model, 800 GeV/c protons strikes a 0.6 inch radius steel cylinder. The cylinder is surrounded by 2.4 inches of air, which is surrounded by 22.3 inches of steel, which is surrounded by 16 inches of concrete. This concrete is surrounded by 10 cm of soil. Refer to figure 9. The model is 10 feet long. Cylindrical symmetry was used to increase statistics. The model is cut into 50 cm long slices (in order to determine the area of maximum star density). The distance to the aquifer is assumed to be 46 feet.

The predicted star density in soil is  $(1.05 \pm 0.11) \times 10^{-6} \text{ stars/cm}^3/\text{proton}$ . Assuming an integrated intensity of  $6.55 \times 10^{16}$  protons per year results in 10% of the allowed tritium limit<sup>8</sup>.

---

<sup>5</sup>private communication, Roger Zimmermann.

<sup>6</sup>private communication, Ross Doyle.

<sup>7</sup>private communication, Roger Zimmermann.

<sup>8</sup>private communication, Roger Zimmermann.

### 4.3 Site Boundary Muons

During the previous fixed target run, the ES&H section conducted onsite and offsite muon measurements. No dose from the MT beamline was reported<sup>9</sup>.

### 4.4 Other Meson Beamlines

To guard against spray being transported down the MPolarized [MP] beamline, no MP devices will be energized. Furthermore, two aluminum billets, each approximately 3 feet long and one foot in diameter, will be placed in the MP beamline in enclosure M03. Finally, the MP beamstop will be driven into the beamline and disconnected.

The shielding around the absorber completely occludes the ME beamline. Furthermore, MEast will not be energized, precluding transport of spray.

MCenter [MC] saw no spray from the MW/MT beamline during the 1996 fixed target run. Even when the MW beam was dumped, spray was not an issue<sup>10</sup>. The current geometry is similar to that of MW dumping on the Meson Train (although the current configuration places the beam farther from, and at a greater angle to MC). Thus, no impact on MC is expected.

The MWest beamline is disabled. As during last run, the MW pinhole collimator has been plugged and disabled; the MW beamstop has been closed and disabled.

## 5 Results

We define our figure-of-merit to be the number of pions at the experiment divided by the number of protons incident on the target. This figure is calculated by multiplying the “Overall Factor” from table 1 by the transmission for the total region listed in table 2 or table 4. For the small-spot mode, this value is  $7.23 \times 10^{-6}$ , while for the large-spot mode it is  $13.3 \times 10^{-6}$ .

This figure is measured in the beamline by dividing the MT6SC1 by MW1SEM. MW1SEM is a secondary emission monitor which is located in front of the primary target—this device measures the proton intensity. MT6SC1 is a pair of 10 cm by 10 cm scintillators, in coincidence, located approximately 55 feet downstream of the final bend. The synthetic device, MTRATIO1, was defined as MT6SC1/MW1SEM, and read at T6 (end-of-spill).

### 5.1 Small Spot

A figure-of-merit for the 150 GeV/c small-spot mode of  $1.36 \times 10^{-5}$  was achieved when taking single-beam to MTest. However, the same configuration gave a figure-of-merit of  $9.17 \times 10^{-7}$  with primary beam split between MCenter and

---

<sup>9</sup>ES&H memo from Kamran Vaziri and Nancy Grossman, dated March 18, 1998

<sup>10</sup>private communication, Catherine James.



MTest—a factor of 13. The probable cause for this is MW1SEM reading too high due to spray from the split.<sup>11</sup>

## 5.2 Large Spot

A figure-of-merit for the 227 GeV/c large-spot mode of  $1.45 \times 10^{-6}$  was consistently measured while splitting primary beam between MTest and MCenter. Measurements were not made with beam only to MTest. Assuming the two-way split causes MW1SEM to over-count by a factor of 13, the adjusted figure would be  $19 \times 10^{-6}$

The ratio of figure-of-merit for 227 GeV/c and 150 GeV/c was measured to be 1.47. Compare this to the calculated value of 1.64.

## 5.3 Purity

Data on particle purity was obtained from T912. For these runs, the small-spot mode was used, with the last two quadrupoles adjusted to focus the beam on the experimental apparatus located in MT6S2.

The following is from Y. Fujii:<sup>12</sup>

**Pion tune:** Beam composition and single-particle fraction are rather stable and do not have strong energy dependence.

- $e \approx 10 - 20\%$ .
- $\mu \approx 5\%$ .
- $\pi$  (or the rest)  $\approx 80\%$ .
- Single-particle fraction  $\approx 50\%$ .

**Electron tune:** Characteristics of e-tune is beamline parameter dependent, even though you set parameters to the same energy. [Authors note: this alludes to the previously mentioned problem of incorrect MW1SEM readings due to spray from the Meson split.]

- Electron fraction is very high (90%) except for the highest energy.
- Single-particle fraction is very low (10%).

For T912, the electron beam was produced by targeting 227 GeV/c pions on MT3CON1 or MT3CON2, and setting the remainder of the beam as documented by R. Tokarek for the 1997 fixed target run. Table 8 shows typical electron rates and purities at three different momenta.

---

<sup>11</sup>This conclusion is consistent with variations seen between an upstream and downstream SEM in the MCenter beamline.

<sup>12</sup>private communication, Yoshiaki Fujii, 6 Oct 99.

For T913, two Cerenkov counters were operational. This, along with the test apparatus, allowed for better particle identification. The electron beam was produced by targeting 227 GeV/c pions on MT3CON1 and setting the remainder of the beamline to the values tabulated in this memo. The electron rate was comparable to that seen in T912, but the single-particle fraction increased to at least 50%. Electrons in the range of 3 to 10 GeV/c were also obtained by transporting 227 GeV/c pions to MT4CON, and using MT5E to select the momentum. This resulted in a larger momentum bite (on the order of 10%) and an electron rate of approximately 1 Hz.

## 6 Conclusion

The beamline performed approximately as predicted. It clearly has much flexibility and many modes of operation that have not yet been investigated. There is every reason to believe that it could operate successfully with 120 GeV/c protons incident on the production target.

## 7 Tables and Figures

Quantity	Value	Units
Production	$2.39 \times 10^{-2}$	pions per proton
Momentum Bite Adjustment	4.8/20	TURTLE bite/MARS bite
Loss due to Decay	7%	(number)
Overall Factor	$5.56 \times 10^{-3}$	(overall factor)

Table 1: Factors used to turn results of TURTLE run into actual transmission.

Region	Transmission
total	$1.3 \times 10^{-3}$
2" $\times$ 2"	$1.3 \times 10^{-3}$
1" $\times$ 1"	$1.1 \times 10^{-3}$
1/2" $\times$ 1/2"	$6.5 \times 10^{-4}$

Table 2: Small-spot mode transmission results from TURTLE run. “Region” refers to a square area normal to the central ray and located in MT6S1. For this run 1,000,000 rays were traced. Recall that this mode is good only to 150 GeV/c.

Element	Current [amp]	Field(Gradient) [kg] ([kG/in])	Type
MT2Q1	53.812	(-2.81)	3Q120
MT2WD1	661.815	6.93	EPB
MT2Q2	46.726	(2.44)	3Q120
MT2WD2	428.3	6.59	6-3-120
MT2V	0	0	4-4-30
MT2WU	718.160	7.52	EPB
MT3Q1	23.172	(-1.21)	3Q120
MT3Q2	21.257	(1.11)	3Q120
MT3V	0	0	4-4-30
MT3SW	0	0	EPB
MT3W	367.675	3.85	EPB
MT3U	33.833	2.10	3D120
MT4Q1			3Q120
MT4Q2			3Q120
MT5V	0	0	4-4-30
MT5Q1	69.132	(3.61)	3Q120
MT5Q2	72.700	(-3.77)	3Q120
MT5E	701.925	7.35	EPB

Table 3: Small spot mode, 120 GeV/c tune. Currents and fields (or gradients) of magnets in the MT beamline.

Region	Transmission
total	$2.4 \times 10^{-3}$
2" × 2"	$1.4 \times 10^{-3}$
1" × 1"	$6.5 \times 10^{-4}$
1/2" × 1/2"	$2.0 \times 10^{-4}$

Table 4: Large-spot mode transmission results from TURTLE run. “Region” refers to a square area normal to the central ray and located in MT6S1. For this run 1,000,000 rays were traced. Recall that this mode is for momentum above 150 GeV/c.

Beam Energy	pi+	pi-	K+	K-	p+	p-
10 GeV	0.68E+05	0.31E+05	0.59E+04	0.50E+04	0.19E+04	0.24E+04
20 GeV	0.20E+06	0.11E+06	0.19E+05	0.16E+05	0.78E+04	0.75E+04
30 GeV	0.34E+06	0.20E+06	0.34E+05	0.28E+05	0.18E+05	0.13E+05
40 GeV	0.48E+06	0.31E+06	0.49E+05	0.39E+05	0.33E+05	0.19E+05
50 GeV	0.59E+06	0.41E+06	0.63E+05	0.48E+05	0.52E+05	0.23E+05
60 GeV	0.70E+06	0.51E+06	0.76E+05	0.56E+05	0.77E+05	0.27E+05
70 GeV	0.81E+06	0.60E+06	0.87E+05	0.62E+05	0.11E+06	0.29E+05
80 GeV	0.91E+06	0.67E+06	0.98E+05	0.67E+05	0.14E+06	0.31E+05
90 GeV	0.10E+07	0.74E+06	0.11E+06	0.71E+05	0.19E+06	0.32E+05
100 GeV	0.11E+07	0.79E+06	0.12E+06	0.74E+05	0.23E+06	0.32E+05
110 GeV	0.12E+07	0.84E+06	0.13E+06	0.76E+05	0.29E+06	0.32E+05
120 GeV	0.14E+07	0.87E+06	0.14E+06	0.78E+05	0.35E+06	0.32E+05
130 GeV	0.15E+07	0.90E+06	0.15E+06	0.79E+05	0.43E+06	0.31E+05
140 GeV	0.16E+07	0.93E+06	0.16E+06	0.80E+05	0.50E+06	0.30E+05
150 GeV	0.17E+07	0.94E+06	0.17E+06	0.80E+05	0.59E+06	0.29E+05
160 GeV	0.18E+07	0.96E+06	0.18E+06	0.81E+05	0.69E+06	0.28E+05
170 GeV	0.19E+07	0.96E+06	0.19E+06	0.81E+05	0.80E+06	0.27E+05
180 GeV	0.20E+07	0.97E+06	0.20E+06	0.80E+05	0.91E+06	0.26E+05
190 GeV	0.21E+07	0.97E+06	0.21E+06	0.79E+05	0.10E+07	0.24E+05
200 GeV	0.22E+07	0.97E+06	0.22E+06	0.78E+05	0.12E+07	0.23E+05
210 GeV	0.23E+07	0.97E+06	0.23E+06	0.77E+05	0.13E+07	0.22E+05
220 GeV	0.23E+07	0.96E+06	0.24E+06	0.75E+05	0.15E+07	0.21E+05

Table 5: Projected rates in MT6S1 for various species and momenta, using the Malensek parameterization. Assumes a 0.7% by 0.4 mradian zero-degree secondary beam, and  $1 \times 10^{11}$  protons per pulse.

Mode	Zone	Rate [kHz]
Large Spot	Total	65 kHz
	2 inch by 2 inch	38 kHz
	1 inch by 1 inch	18 kHz
	1/2 inch by 1/2 inch	6 kHz
Small Spot	Total	36 kHz
	2 inch by 2 inch	36 kHz
	1 inch by 1 inch	31 kHz
	1/2 inch by 1/2 inch	18 kHz

Table 6: Projected rates in MT6S1 for large-spot and small-spot modes. Assumes  $1.0 \times 10^{11}$  protons per pulse on target and a 20 second spill time.

location	Beam Momentum (GeV/c)							
	227	120	60	8	-8	-60	-120	-227
MT2Q1	0.0	0.0	0.0	0.0	0.0	0.0	0.0	0.0
	0.0	0.0	0.0	0.0	0.0	0.0	0.0	0.0
MT2WD1-1	0.0	0.0	0.0	0.0	0.0	0.0	0.0	0.0
	-5.8	-6.8	—	—	—	—	—	-10.3
MT2Q2	-6.9	-8.2	—	—	—	—	—	-12.4
	-17.2	-20.5	—	—	—	—	—	-30.9
MT2WD1-2	-18.1	-21.5	—	—	—	—	—	-32.5
	-32.6	-38.7	—	—	—	—	—	-58.5
MT2WD1-3	-48.9	-58.0	—	—	—	—	—	-87.6
	-74.3	-88.9	—	—	—	—	—	-134.3
ABSORBER	-78.3	-92.9						-140.4
	-110.1	-130.7						-197.3

Table 7: Separation between primary beam and secondary beams of various momenta at upstream and downstream face of element. Negative momenta indicate negatively charged beam. All units are millimeters. The beam pipe is 3 inches in diameter, implying primary beam exits pipe when separation exceeds 38.1 mm.

Momentum GeV/c	Electron Rate [Hz]	Purity [percent]
150	87	44
100	110	55
50	111	56

Table 8: Electron rate and purity using the T912 configuration. Recall that the single particle fraction is approximately 10%, so the usable electron rate is much lower. Rates are normalized to  $1 \times 10^{11}$  protons per 40 second spill on target.

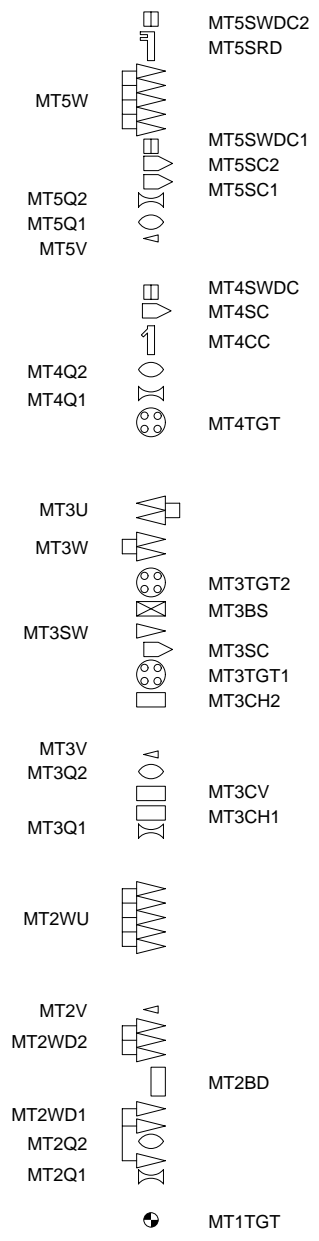
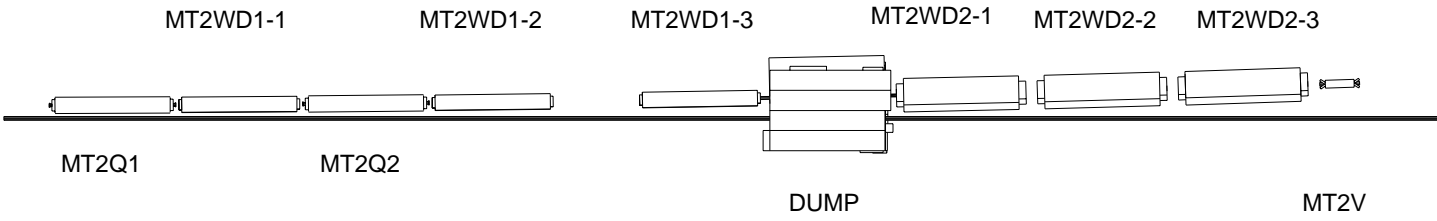


Figure 1: Schematic diagram of MTest beamline, showing magnets and other components.



16

Figure 2: Plan view of upstream end of M02 showing MTtest beamline elements.



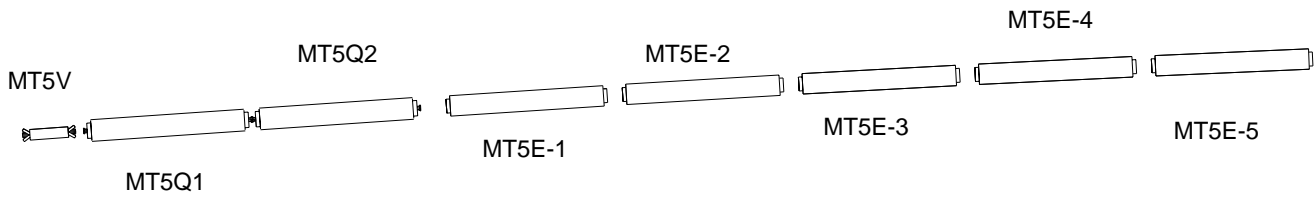


Figure 3: Plan view of upstream end of MT5 showing MTest beamline elements.

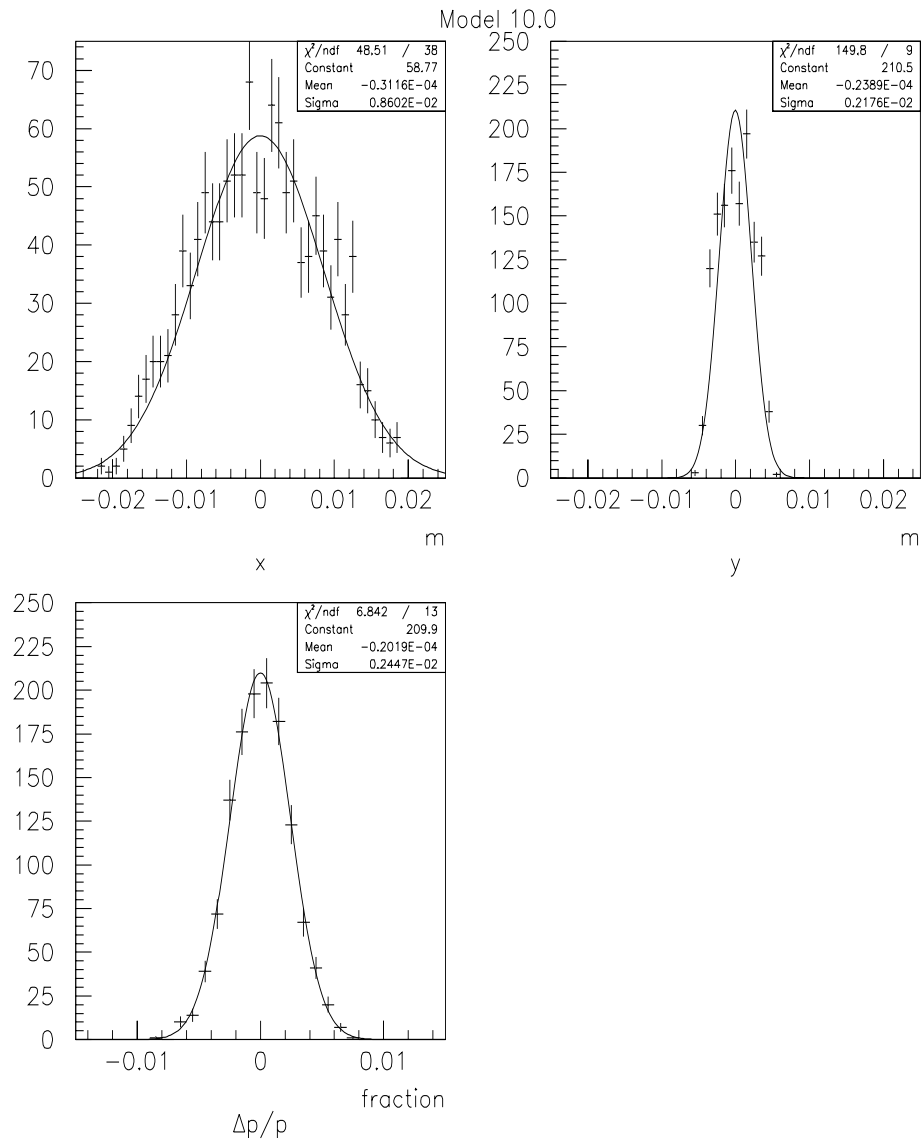


Figure 4: "Small-spot" mode. Pion beam profiles and spectrum at the approximate location of the BTeV detector.

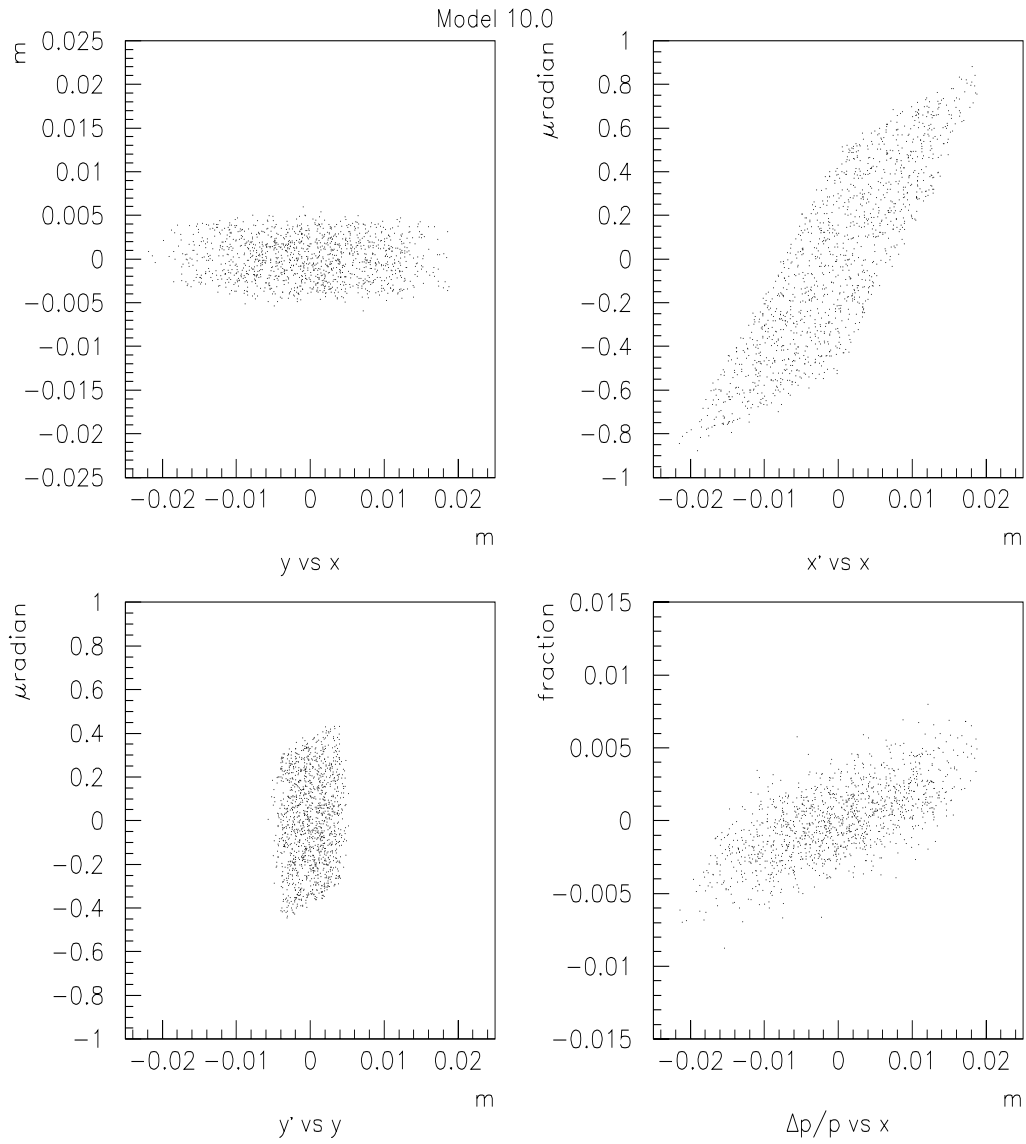


Figure 5: "Small-spot" mode. Beam spot, phase space, and dispersion of the pion beam at the approximate location of the BTeV detector.

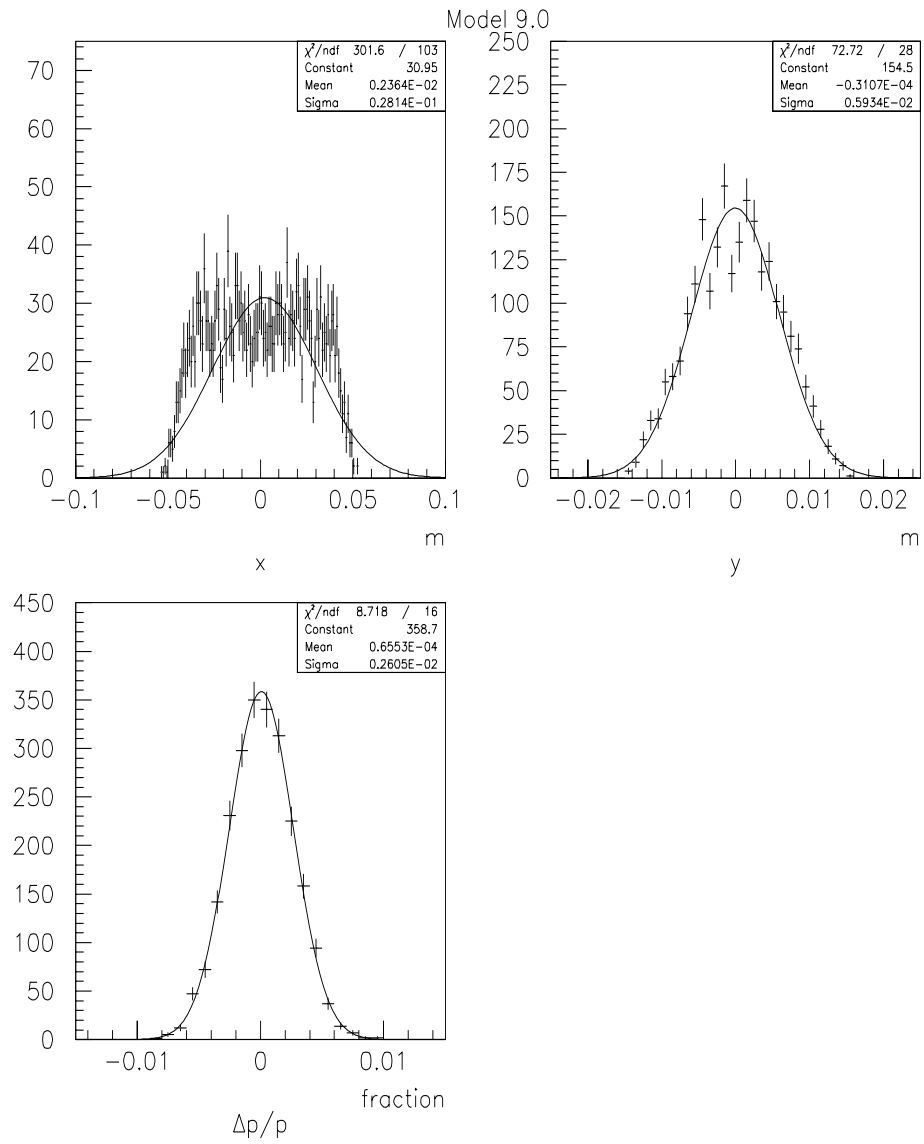


Figure 6: "Large-spot" mode. Pion beam profiles and spectrum at the approximate location of the BTeV detector.

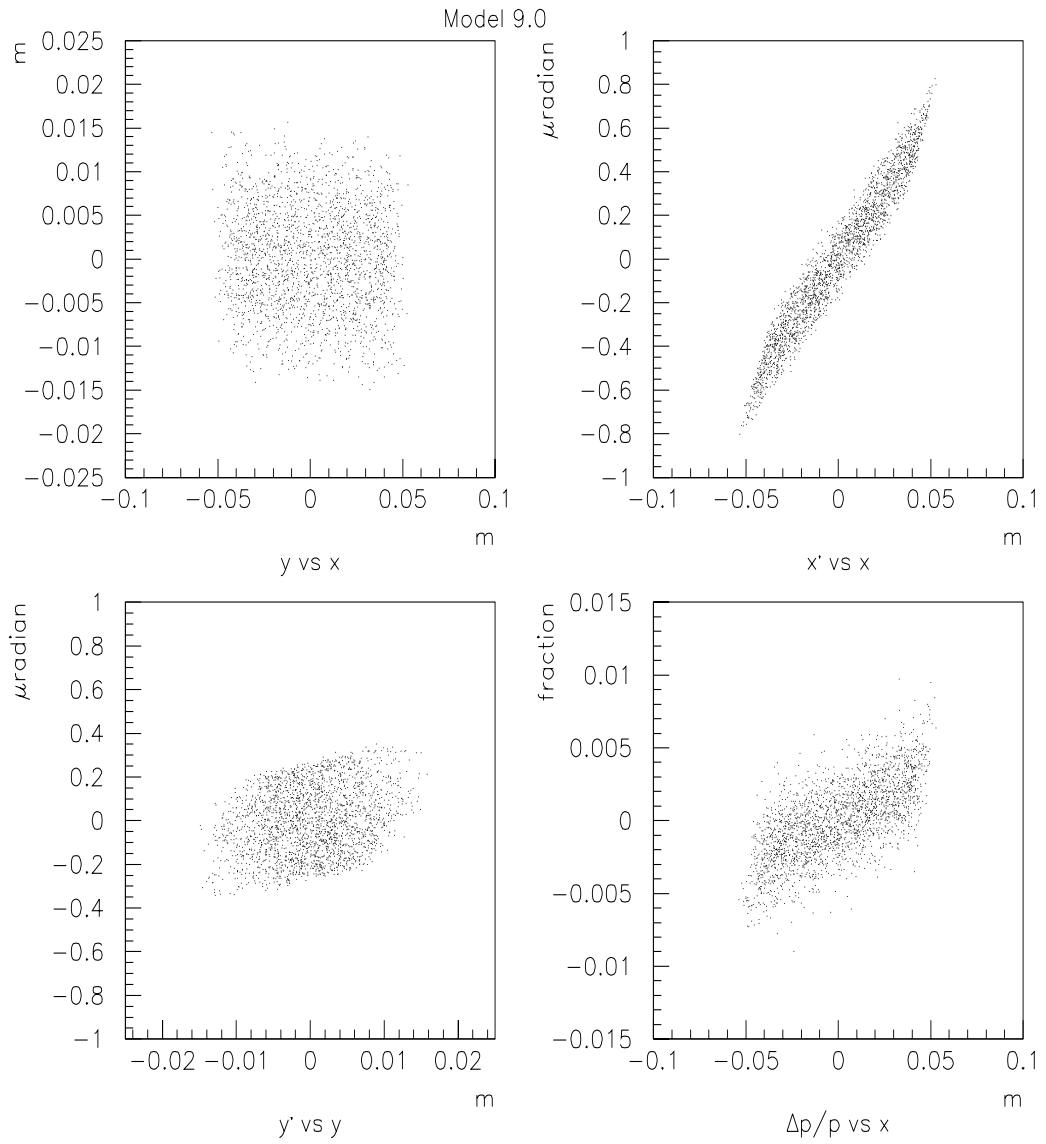


Figure 7: "Large-spot" mode. Beam spot, phase space, and dispersion of the pion beam at the approximate location of the BTeV detector.

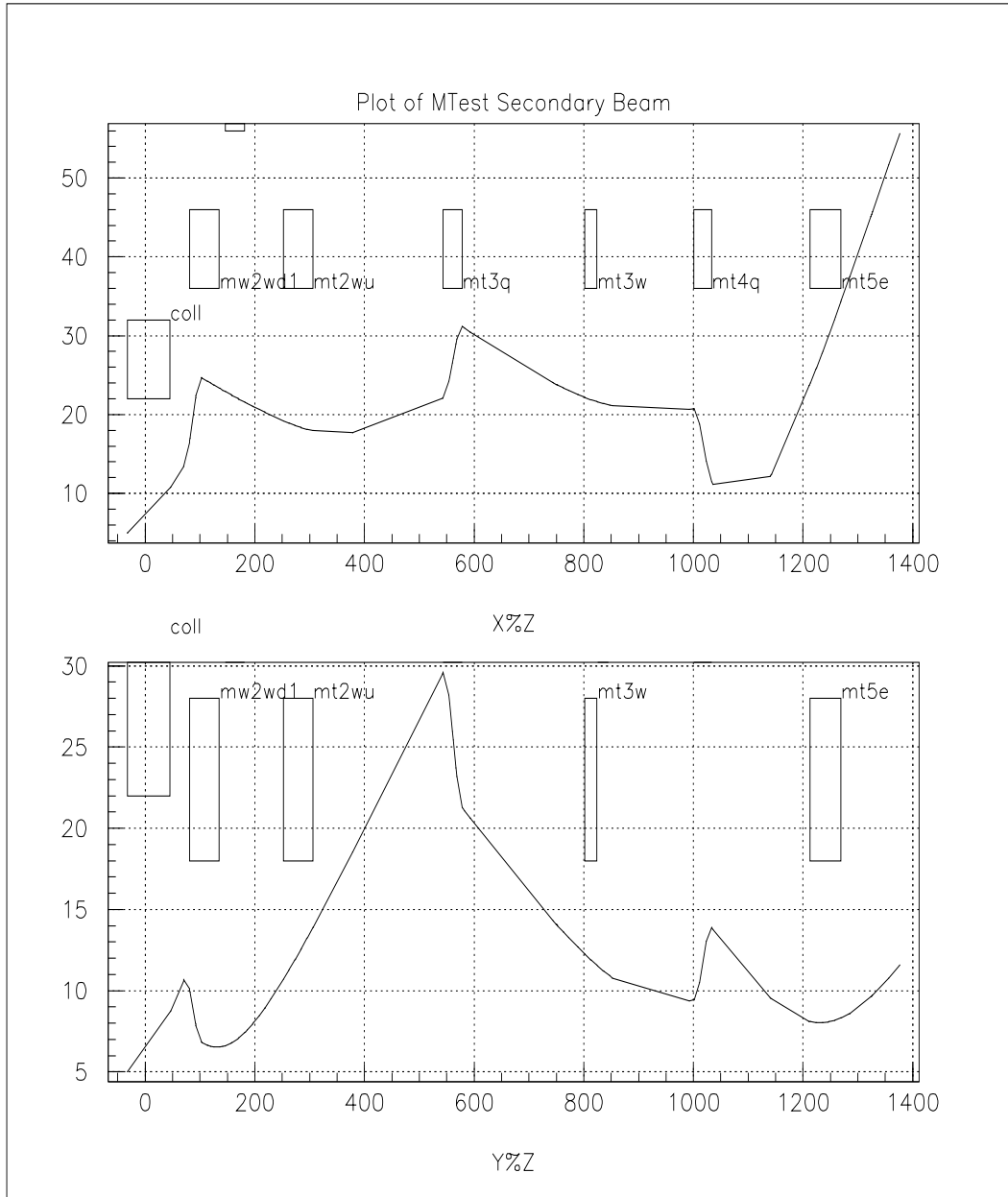
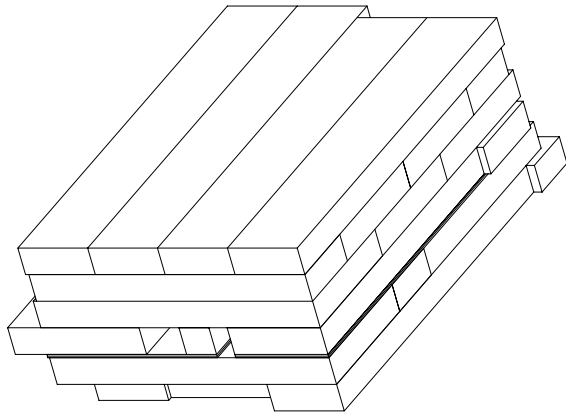


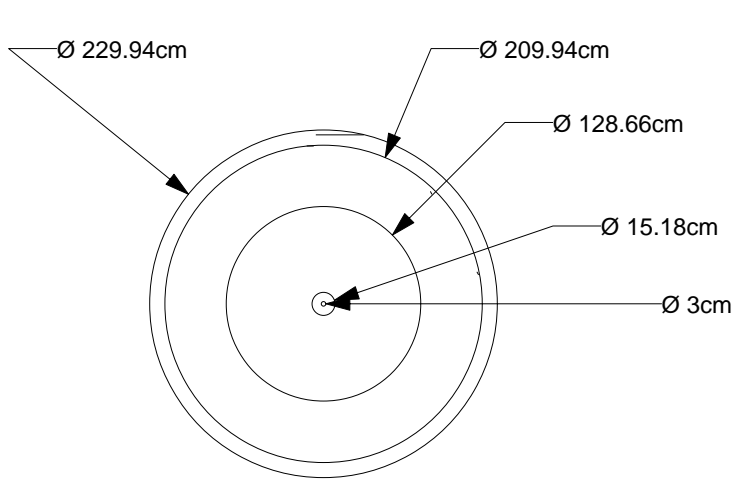
Figure 8: Horizontal and vertical beam envelope. This is the same beam as assumed for the Malensek parameterization.



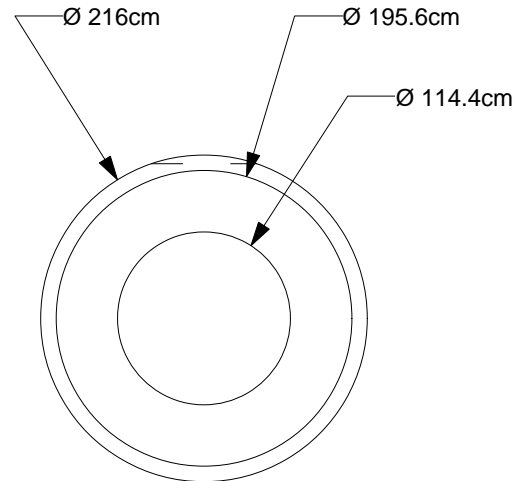
(a)



(b)



(c)



(d)

Figure 9: (a) Three-dimensional view of MT absorber and shielding. (b) Front face of absorber and shielding (beam is into page). (c) Geometry used to model soil activation in least-iron case. (d) Geometry used to model soil activation in greatest-iron case.